



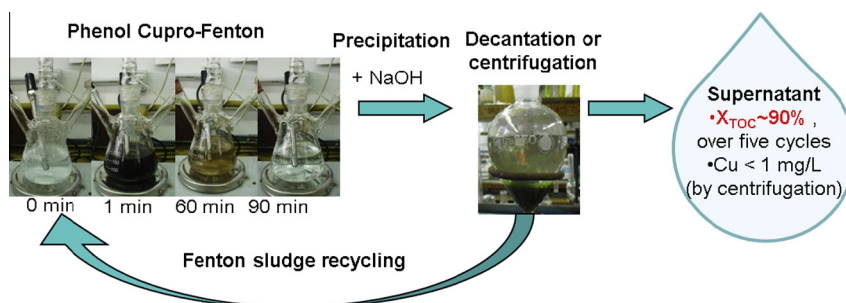
Catalyst reutilization in phenol homogeneous cupro-Fenton oxidation

N. Inchaurredo^{a,*}, E. Contreras^b, P. Haure^a^aDpto. de Ingeniería Química, Div. Catalizadores y Superficies – INTEMA – CONICET, Universidad Nacional de Mar del Plata, Mar del Plata 7600, Argentina^bDiv. Catalizadores y Superficies – INTEMA – CONICET, Universidad Nacional de Mar del Plata, Mar del Plata 7600, Argentina

HIGHLIGHTS

- Phenol can be efficiently mineralized by the homogeneous cupro-Fenton reaction.
- A lumped kinetic model adequately represents TOC, phenol and H₂O₂ profiles.
- The homogeneous catalyst is recovered and reused in subsequent reactions.

GRAPHICAL ABSTRACT



ARTICLE INFO

Article history:

Received 15 December 2013

Received in revised form 4 April 2014

Accepted 5 April 2014

Available online 19 April 2014

Keywords:

Phenol mineralization

Homogeneous cupro-Fenton

Sludge reutilization

ABSTRACT

The catalytic wet peroxide oxidation of phenol (1 g/L) was performed in a laboratory batch reactor using the cupro-Fenton homogeneous reaction. At 70 °C and using 200 mg/L of Cu (II) complete phenol removal, high TOC reduction (ca. 85%) and efficient use of hydrogen peroxide were achieved. A lumped kinetic model that accounts for organics mineralization and peroxide consumption was developed to predict reactants and total organic carbon profiles. After the reaction step, Cu(II) was recovered by precipitation with NaOH; Cu(II) concentration in the discharged liquid was always less than the 1 mg/L. The sludge was reused in subsequent reaction steps with minor fluctuations in the catalytic activity. The combination of the cupro-Fenton reaction with an alkaline precipitation procedure allows lower operational costs and helps to reduce the toxicity of the treated wastewater.

© 2014 Elsevier B.V. All rights reserved.

1. Introduction

Effluents containing phenolic compounds can be effectively treated by the Fenton process. This method consists in the reaction of Fe(II) species with H₂O₂ under acidic conditions to generate highly oxidizing hydroxyl radicals (HO·) [1]. Although this process presents several advantages over other oxidation techniques [2,3], one major drawback is that the Fenton reaction is effective within a narrow pH range (e.g., pH 3–4) while most wastewaters have pH values ranging from 5 to 7 [4].

Several researchers suggested the use of other transition metals such as copper, ruthenium, cerium, and manganese. These metals can also promote the generation of hydroxyl radicals from H₂O₂ in a wide-working pH range (pH 3–7) [5]. Mantzavinos [6] studied oxidation of derivatives of the cinnamic acid comparing the behavior of Cu(II) and Fe(II) as catalysts for the Fenton reaction. Both cations proved to be effective in the oxidation reaction, but at higher temperatures Cu(II) increased its effectiveness compared to Fe(II). Mantzavinos [7] also studied the Fenton oxidation of a synthetic effluent containing benzoic acid derivatives with Cu(II) and Fe(II); Mantzavinos reported that the classical Fenton reagent (Fe(II)/H₂O₂) was less effective than Cu(II)/H₂O₂ system measured in terms of mineralization at high temperatures. Nichela et al. [8] reported that the reduction of the total organic carbon (TOC) was

* Corresponding author. Tel.: +54 2234816600 242; fax: +54 2234810046.

E-mail address: ninchaurredo@gmail.com (N. Inchaurredo).

higher in Cu(II) than in Fe(III)-based systems for the nitrobenzene oxidation by hydrogen peroxide in homogeneous systems. Castro et al. [9] demonstrated that at 30 °C, Cu(II) was active to the oxidation of phenol; even at low copper concentrations (5 mg/L) and using the stoichiometric amount of H₂O₂ (14 mol/mol) those authors obtained a 15% conversion of phenol in 2 h. Prasad et al. [10] successfully used copper salts in homogeneous reaction with H₂O₂ and O₂ as oxidizing agents for the treatment of petrochemical wastewaters. Recently, Friedrich et al. [11] studied the effect of the addition of Cu(II) ions to the classical Fenton reaction for the oxidation of phenol. In the reaction with Fe(II)/Fe(III), the presence of aliphatic organic acids (mainly oxalic acid) resulted in a high final TOC value; however, the addition of Cu(II) increased the TOC conversion. All these reports suggest that Cu(II) could be a suitable candidate to replace the Fe(II) in the Fenton reaction.

One of the main problems concerning the use of copper as the catalyst for the Fenton reaction is related with its well-known toxicity [12,13]. To overcome this problem, the oxidation treatment should be followed by a Cu(II) separation step, such as precipitation; additionally, recycling the Cu(II) also reduces the operation costs. Precipitation by hydroxide formation is the most common method for heavy metal recovery. The precipitate obtained after the alkalization of the reaction media is often called the Fenton sludge. Cao et al. [14] investigated the recycling of Fenton sludge; those authors dewatered, dried and heated the sludge at 350–400 °C for 20–30 min and the residual solids were dissolved in sulfuric acid to form a reusable Fe catalyst. The recovered catalyst was highly effective for the oxidative pretreatment of a fine chemical wastewater. Therefore, alkaline precipitation and recycling of Cu(II) could be a viable alternative for the cupro-Fenton process.

The knowledge of the oxidation kinetics is a key feature for the accurate design of a wastewater treatment process. Available kinetic models for the classic Fenton process vary in complexity. The simplest models use empirical kinetic expressions to represent the experimental data [15–19]. Some researchers suggested simplified reaction mechanisms and proposed lumped models in which organic compounds are grouped according to their susceptibility to oxidation [20,21]. Finally, detailed models described in terms of elementary reactions are also available [22–24]. For example, Kang et al. [24] proposed a kinetic model for Fenton oxidation of phenol and monochlorophenols that considers 28 reactions. Although these detailed models are useful for the accurate prediction of the reaction intermediates, their complexity also hampers its application for practical purposes. Moreover, this kind of analysis is more difficult in systems with copper due to the lack of kinetic constants reported for the Fenton process with this cation.

Up to the present, only few publications deal with homogeneous Fenton processes with copper as catalyst, and only one reports specifically the application of this system to the degradation of phenol [9]. For this reason, the objective of this study was to investigate the capability of Cu(II) as a Fenton-like catalyst for the oxidation of phenol as a model pollutant. The effect of the copper precursors, temperature, and concentrations of copper and H₂O₂ on the conversions of phenol, TOC, and H₂O₂ was studied. A kinetic model was proposed to describe the abatement of phenol, H₂O₂ and TOC under the different tested conditions. The reutilization of the cupro-Fenton sludge was also studied in a cupro-Fenton sequencing batch reactor (CF-SBR).

2. Experimental

2.1. Oxidation of phenol solutions in cupro-Fenton batch reactors

In a typical experiment, a specific amount of a copper salt was dissolved into 170 mL of 1 g/L phenol aqueous solution (p.a.,

Cicarelli, Arg.) in a 250 mL thermostated batch reactor provided with vigorous agitation (800 rpm). When the reaction temperature was reached, a given volume of 30 wt.% hydrogen peroxide (Cicarelli, Arg.) was added into the system and the reaction started. In all cases the initial pH was between 5.0 and 6.0; this pH value was due to the hydrolysis of Cu(II) and the slightly acid characteristic of phenol and hydrogen peroxide. At different time intervals samples were withdrawn and promptly analyzed to determine pH, phenol, hydrogen peroxide and total organic carbon (TOC) concentrations. During the reaction, pH was monitored but not controlled because its evolution was considered as an indication of the presence of acidic intermediates [19,25]. In order to select the most appropriate reaction conditions, experiments were performed varying the Cu(II) precursors, temperature, and catalyst and H₂O₂ concentrations.

2.2. Effect of operation conditions on the cupro-Fenton oxidation of phenol

Different copper precursors, Cu(NO₃)₂·2.5H₂O (p.a., Riedel-de Haën, Germany); CuCl₂·2H₂O (p.a., Cicarelli, Arg.) and CuSO₄·5H₂O (p.a., Biopack, Arg.) were tested. In these experiments, various amounts of cupric salts were used to obtain a total copper concentration (Cu_T) of 100 mgCu/L. In all cases, T = 50 °C, and initial hydrogen peroxide and phenol concentrations were 190 mM, and 10.6 mM, respectively.

The effect of the initial hydrogen peroxide on the oxidation of phenol solutions (10.6 mM) was also studied. In these experiments, tested values corresponding to the ratio (R) between the initial H₂O₂ concentration and the theoretical stoichiometric amount of hydrogen peroxide (14 mol/mol) for the complete oxidation of phenol ranged from 0.5 to 1.5. This range is usually studied by other authors [26–29]. The effect of the catalyst concentration (5–800 mgCu/L) on the oxidation of phenol solutions (10.6 mM) was tested at 30, 50 and 70 °C; in these experiments R was 1.3, and initial pH = 5.

2.3. Operation of a cupro-Fenton sequencing batch reactor (CF-SBR)

The CF-SBR had 170 mL of working volume (V₀) to perform the following operations: filling with a given volume (V_S mL) of the phenol stock solution, heating to the operation temperature (50 or 70 °C), addition of hydrogen peroxide to start the reaction step (90 or 240 min), cooling in a water bath to room temperature (30 min), addition of drops of NaOH (1 M) for copper precipitation followed by a sedimentation or a centrifugation step, and extraction of a volume of the supernatant equivalent to V_S (e.g., the treated effluent). In the initial test, 0.136 g of CuSO₄·5H₂O was added to the phenol solution to obtain 200 mg/L of Cu(II) in the reaction solution. Once the reactor reached a desired temperature, the oxidant was added. When sedimentation was used to recover the cupro-Fenton sludge, the extracted volume (V_S) was 80 mL; when centrifugation was used, V_S = 140 mL. Then, a volume of the phenol stock solution equivalent to V_S was added to the remnant volume (V₀ – V_S) in the reactor that contained the precipitated Cu(II). The precipitated cupro-Fenton sludge was dissolved by the addition of a few drops of concentrated sulfuric acid; then, the next operation cycle started with the addition of the hydrogen peroxide stock solution. In all the experiments, phenol and peroxide concentrations at the beginning of the reaction phase were 10.6, and 190 mM, respectively. However, due to copper losses during the recycling of the cupro-Fenton sludge, the total copper concentration (Cu_T) decreased as a function of the operation cycle. Moreover, because part of the TOC at the end of the reaction time was also precipitated during the addition of NaOH, the initial TOC of each reaction phase was a mixture comprised by the added phenol and the remnant TOC corresponding to the previous cycle.

2.4. Analytical methods

pH was determined using a Black Stone pH controller.

Phenol concentrations were measured using the 4-aminoantipyrene method [30]; calibration curves were performed periodically using phenol as the reference compound. The 4-aminoantipyrene method determines phenol, ortho- and meta-substituted phenols. Phenolic compounds with a substituent in the para position may not quantitatively produce color with 4-aminoantipyrene. However, para substituents of phenol such as carboxyl, halogen, methoxyl, or sulfonic acid groups can produce color with 4-aminoantipyrene under proper conditions [30]. Solutions of 500 mg/L of p-benzoquinone, hydroquinone and catechol were analyzed by the 4-aminoantipyrene method. Only catechol can be considered as a possible interference in the phenol determination; however, the absorbance corresponding to catechol was 0.16 times the value corresponding to phenol at the same molar concentration.

Hydrogen peroxide concentration was measured by a iodometric titration method [30]. Total organic carbon (TOC) was determined in a TOC analyzer (Shimadzu, model TOC-VCPN). Total copper concentration (Cu_T) was measured using a commercial kit (CuVer 2™, Hach). Reported values are the average of at least two measurements, and error bars represent the standard deviation.

2.5. Estimation of the model coefficients and dynamic simulations

Calculation of coefficients of the mathematical model proposed in this work and the dynamic simulations were performed using the software package Gepasi 3 [31]. The LSODA routine (Livermore Solver of Ordinary Differential Equations) was selected to solve the system of differential equations of the model developed in the present work. The Multistart Optimization algorithm (with Levenberg–Marquardt local optimization) was selected to fit the proposed model to the experimental data.

3. Results and discussion

3.1. Effect of the copper precursor

In the first set of experiments, cupric sulfate, nitrate and chloride were used as the source of Cu(II). In all cases, results obtained using these cupric salts were quite similar. For example, conversions corresponding to TOC (X_{TOC}), H_2O_2 ($X_{H_2O_2}$), and phenol (X_{Phenol}) at 180 min using the three tested cupric salts were around 60%, 70%, and 100%, respectively. In all cases pH dropped from 5 to 3 within the first 15 min and then it remained almost constant. A similar trend of pH as a function of time was obtained for all the assays performed in this work (Supplementary data, Figs. SD1 and SD2).

Pignatello et al. [32] reported that the presence of inorganic ions could interfere in the Fenton process as follows: (i) complexing Cu(I) and Cu(II) ions, which would affect the catalytic activity of copper, (ii) precipitation, (iii) radical elimination or formation of less active radical species, and (iv) oxidation reactions involving inorganic radicals. However, the effect of the inorganic ions depends on the concentration. Most authors report negative effects considering concentrations of the inorganic ions much higher than the ones employed in this study [33–35]. For example, the inhibition by chloride is noticeable above 0.01 mol/L [32] and the concentration of chloride introduced in this study by adding copper in the form of a chloride salt is much lower (0.003 mol/L). Under the conditions employed in the present work, no differences between the results obtained using different cupric salts were observed, probably due to the low concentrations. Because sulfuric

acid was used to solubilize the precipitated cupro-Fenton sludge (see Section 2.3), in the following tests $CuSO_4 \cdot 5H_2O$ was employed as the Cu(II) source.

3.2. Effect of the initial hydrogen peroxide concentration

One determining factor on the economy and efficiency of the Fenton process is the H_2O_2 consumption. Low peroxide doses may lead to partial treatments; conversely, the excess of peroxide has to be removed before discharging the effluent due to its toxicity [36]. For this reason, the initial H_2O_2 concentration must be carefully selected.

Fig. 1a–c shows the effect of the initial hydrogen peroxide concentration, expressed as the ratio (R) between the initial H_2O_2 concentration and the theoretical stoichiometric amount of peroxide for the complete oxidation of phenol, on the conversions of TOC (X_{TOC}), H_2O_2 ($X_{H_2O_2}$), and phenol (X_{Phenol}). As it was expected, in all cases conversions increased with time. Although $X_{H_2O_2}$, X_{Phenol} were quite similar for all the tested R values, TOC consumption rates and maximum TOC conversions were a function of the ratio R . Fig. 1d shows that while X_{Phenol} at 180 min was close to 100%, X_{TOC} increased with the increment of R ; however, no significant improvement of X_{TOC} occurred for R values higher than 1.3 (190 mmol/L). Within the tested conditions, $X_{H_2O_2}$ was higher than 80%; in this case, a decreasing trend of $X_{H_2O_2}$ as a function of R was obtained (Fig. 1d). These results suggested that the rate of TOC conversion was related with the rate of generation of hydroxyl radicals, which was a function of the hydrogen peroxide concentration [36].

3.3. Effect of temperature and copper concentration

Oxidation assays of phenol solutions (10.6 mM) by the cupro-Fenton reaction were performed at 30, 50 and 70 °C using Cu_T concentrations between 5 and 800 mg/L, and 190 mmol/L of H_2O_2 . Fig. 2 shows that TOC, H_2O_2 , and phenol conversions obtained at 50 °C increased as a function of time and the added Cu_T . Similar results were obtained at 30 and 70 °C. For example, at 30 °C the phenol conversion after 240 min was around 90% but still incomplete, even at the highest catalyst concentration evaluated (200 mg/L). The TOC conversion was quite poor, 22% and 30% for 100 and 200 mg/L, respectively (Figs. 3 and 4).

To achieve higher degrees of mineralization it was necessary to increase the temperature (Fig. 3). At 50 °C, copper is quite active for oxidation of phenol, even at low concentrations. The reaction with 5 mg/L of Cu(II) presented a final phenol conversion of 85%. However, the level of mineralization achieved was low (14%) (Fig. 4). When catalyst concentrations higher than 20 mg/L were employed, a phenol conversion close to 100% was obtained after the first 30 min of reaction. For all temperatures, TOC conversion increased with the catalyst load (Fig. 4). Using $Cu_T = 800$ mg/L at $T = 50$ °C it was possible to obtain a TOC conversion of 80% in 90 min. However, using 200 mg/L at the same temperature, a double of time (240 min) was necessary to achieve the same degree of mineralization.

At $T = 50$ °C, when 800 mg/L of copper was employed, pH dropped sharply to pH 3 within the first 15 min due to the formation of organic acids. Then, because an excess of hydrogen peroxide was used, pH slowly rose due to the mineralization of those acids. With concentrations between 70 and 200 mg/L, the pH maintained slightly above 3, while in the 20–60 mg/L range pH stayed just below 3. When the copper concentration was 5 mg/L, pH reached values below 2.5. In the latter case, these low pH values indicated a high accumulation of carboxylic acids due to the reduced level of mineralization (Supplementary data, Fig. SD2). In summary, at 50 °C when a low Cu_T concentration was employed, a moderate

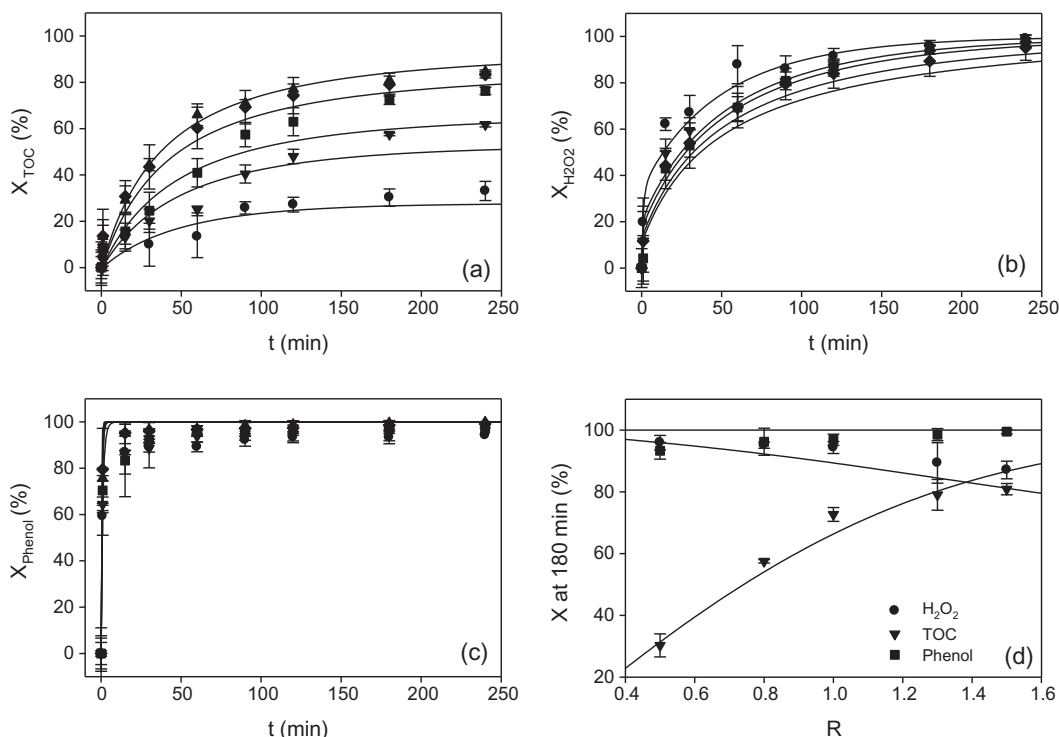


Fig. 1. Conversions (X) of (a) TOC, (b) H_2O_2 , and (c) phenol as a function of time for different initial peroxide concentrations (mM): 74 (circles), 117 (triangles down), 145 (squares), 195 (triangles up), 228 (diamonds). (d) Conversions of TOC, H_2O_2 , and phenol obtained at 180 min as a function of the ratio R . Other experimental conditions: $[\text{Phenol}]_0 = 10.6 \text{ mM}$, $[\text{Cu}_{\text{T}}] = 200 \text{ mg/L}$, $T = 50 \text{ }^\circ\text{C}$, $\text{pH}_0 = 5.0$. In all cases, lines indicate the proposed model (Eqs. (7)–(9)) using the coefficients showed in Table 2.

phenol conversion was achieved, accompanied by a poor mineralization and gradual accumulation of carboxylic acids. By increasing the catalyst load, higher phenol conversions were achieved and the mineralization of the contaminant is promoted. However, the final color of the reaction solution over the whole concentration range was brown (Table 1).

The effect of the Cu_{T} concentration on the oxidation of phenol was also evaluated at $70 \text{ }^\circ\text{C}$. When 5 mg/L of copper was tested, a phenol conversion close to 100% was obtained in only 30 min; however, TOC conversion was about 35%. To achieve an 80% TOC conversion, it was necessary to increase the catalyst concentration up to 60 mg/L . A further increment to 100 or 200 mg/L of $\text{Cu}(\text{II})$, allowed higher TOC conversion rates and final TOC values around 90%, in only 90 min for 100 mg/L and 60 min for 200 mg/L (Figs. 3 and 4). These results indicated the presence of a residual TOC of about 10% of the initial value, which may correspond to the refractory organic acids resistant to the tested cupro-Fenton oxidation conditions [37]. Also, the accumulation of these acids may form complexes with $\text{Cu}(\text{II})$, reducing its activity towards the oxidation [20,38,39].

When copper concentrations between 5 and 20 mg/L were employed at $70 \text{ }^\circ\text{C}$, pH immediately decreased to 3 and then, it remained constant during the reaction time. The evolution of pH for higher concentrations of copper (100 and 200 mg/L) presented an immediate decrease of pH to values about 2.5; then, a gradual increase of pH was observed (Supplementary data, Fig. SD2). This behavior was attributed to an initial fast formation of organic acids followed by their mineralization. In summary, when the temperature was increased up to $70 \text{ }^\circ\text{C}$ in the presence of sufficient mass of catalyst, the decomposition of H_2O_2 into radicals was accelerated. As a result, the mineralization degree was also enhanced and the final pH was higher due to further mineralization of the carboxylic acids produced during the first phase of the phenol oxidation. The final solution was almost colorless (light amber, transparent), even with low copper concentrations (60 mg/L).

Although in all the tested conditions the final phenol conversion was higher than 90%, when combinations of low operation temperatures with low initial hydrogen peroxide or copper concentrations were tested, the final color of the reaction mixture was dark brown. The production of colored wastewaters difficult the implementation of the oxidation treatment; moreover, remaining color could be a sign of the toxicity level [40]. Color generation during phenol oxidation is a fast reaction where the phenolic solution changes initially from colorless to brown. During the first stages of oxidation, highly colored intermediate compounds such as *p*-benzoquinone (yellow) and *o*-benzoquinone (red) are generated [40]. Moreover, it was reported the formation of colored cation complexes and phenol condensation products [41]. This effect was more noticeable when low Cu_{T} concentrations or low temperatures were tested (Fig. 5). However, if the oxidation conditions are adequate, these colored compounds can be further oxidized to give short chain organic acids and carbon dioxide, yielding an almost colorless solution [40]. For this reason, with high Cu_{T} concentrations, or high temperatures the measured phenol conversion was 100%. Table 1 summarized some obtained results.

3.4. Kinetic model for the cupro-Fenton oxidation of phenol

Several authors reported that the oxidation of phenol by AOPs is characterized by an initial fast consumption of oxidants and phenol, producing several intermediates, such as catechol, hydroquinone, *p*-benzoquinone, as well as various organic acids (muconic, malic, fumaric, oxalic). In a second phase, a slow consumption rate of oxidants and intermediates is usually observed due to the low reactivity of some of these intermediates and the complexation of the catalyst by organic intermediates. Numerous reaction pathways for the oxidation of phenol solutions by AOPs have been reported [42–47]. Phenol oxidation can take place at *para* or *ortho*-positions. During the first phase, the oxidation of phenol at

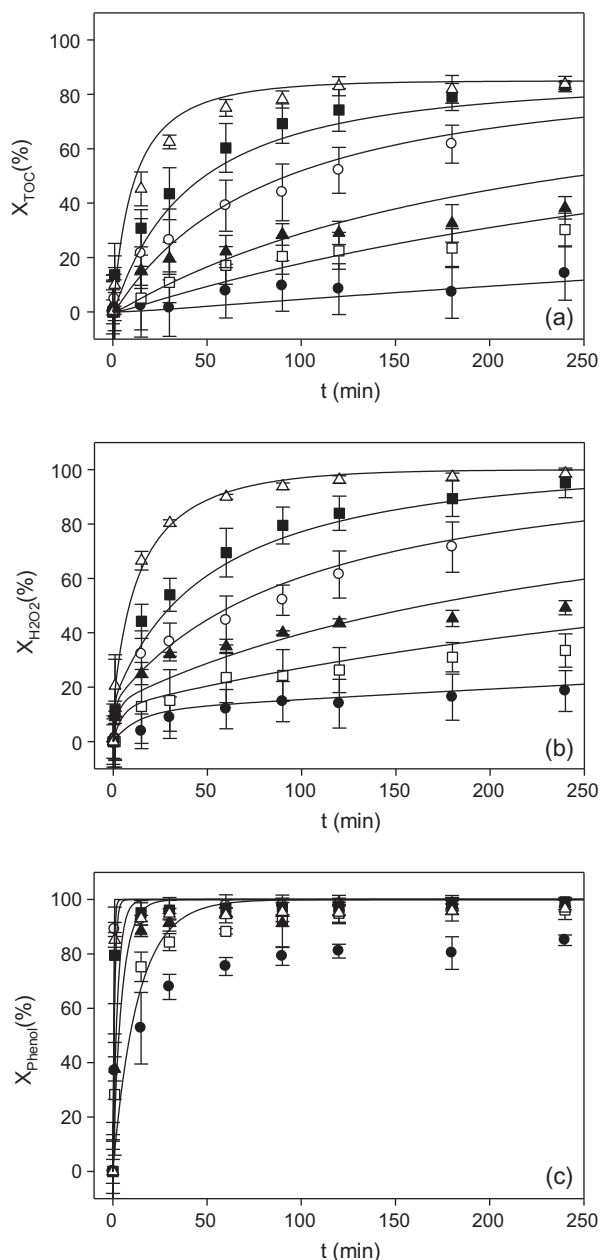
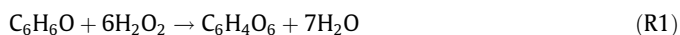
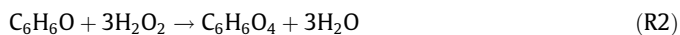


Fig. 2. Conversions (X) of (a) TOC, (b) H_2O_2 , and (c) phenol as a function of time for different Cu_T concentrations (mgCu(II)/L): 5 (full circles), 20 (open squares), 40 (full triangles), 100 (open circles), 200 (full squares), 800 (open triangles). Other experimental conditions: $[Phenol]_0 = 10.6$ mM, $[H_2O_2]_0 = 190$ mM, $T = 50$ °C, $pH_0 = 5.0$. In all cases, lines indicate the proposed model (Eqs. (7)–(9)) using the coefficients showed in Table 2.

the *para*-position generates *p*-benzoquinone which can be further oxidized to give 2,5-dioxo-3-hexenedioic acid ($C_6H_4O_6$):



Alternatively, the oxidation of phenol via the *ortho*-position generates muconic acid ($C_6H_6O_4$):



According to Reactions (1) and (2), during the first phase of the phenol oxidation 3–6 mol of H_2O_2 are consumed per mol of phenol oxidized, being the actual value a function of the reaction conditions (e.g., type of oxidant, temperature, initial concentrations,

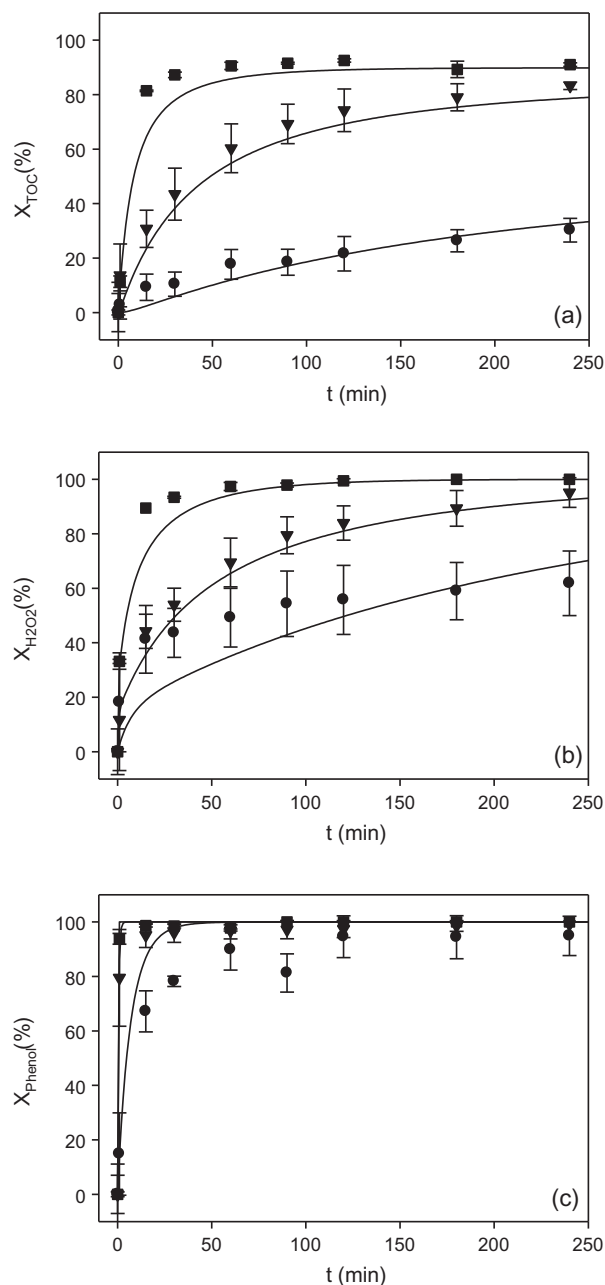


Fig. 3. Conversions (X) of (a) TOC, (b) H_2O_2 , and (c) phenol as a function of time obtained at different temperatures: 30 °C (circles), 50 °C (triangles), and 70 °C (squares). Other experimental conditions: $[Phenol]_0 = 10.6$ mM, $[H_2O_2]_0 = 190$ mM, $[Cu_T] = 200$ mgCu(II)/L, $pH_0 = 5.0$. In all cases, lines indicate the proposed model (Eqs. (7)–(9)) using the coefficients showed in Table 2.

type and concentration of catalyst). However, taking into account that muconic ($C_6H_6O_4$) and 2,5-dioxo-3-hexenedioic ($C_6H_4O_6$) acids are both C_6 -compounds, TOC values remain constant during these reactions.

In the second phase, 2,5-dioxo-3-hexenedioic ($C_6H_4O_6$) and muconic ($C_6H_6O_4$) acids are further oxidized to give a mixture of organic acids, such as 4-oxo-2-butenic, maleic, glyoxylic, and oxalic, and CO_2 . In excess of the oxidant, 4-oxo-2-butenic acid gives glyoxylic, oxalic, and maleic acids. Additionally, these acids can also be oxidized producing acetic and formic acids, and eventually CO_2 [44,47]. The overall stoichiometry corresponding to the oxidation of 2,5-dioxo-3-hexenedioic ($C_6H_4O_6$) or muconic ($C_6H_6O_4$) acids to CO_2 by H_2O_2 is the following

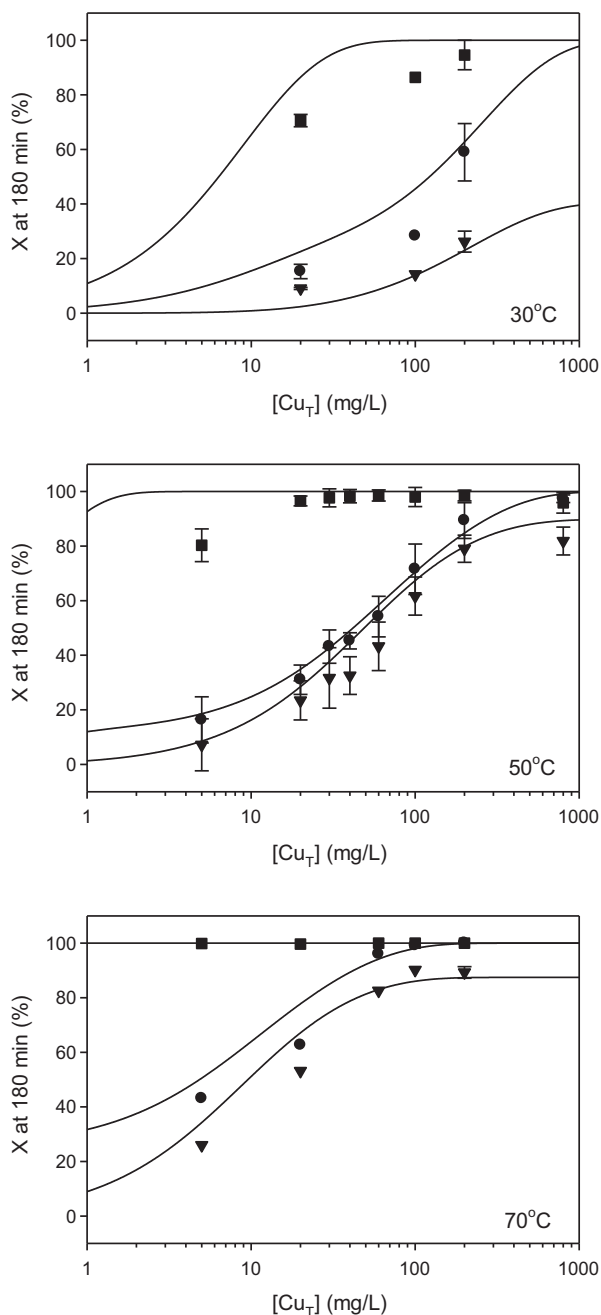
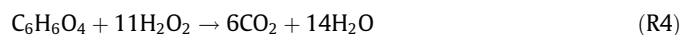
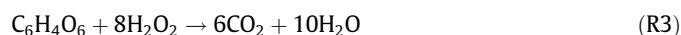
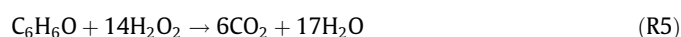


Fig. 4. Conversions (X) of TOC (triangles), H_2O_2 (circles), and phenol (squares) obtained at 180 min as a function of the Cu_T concentration at three different temperatures ($T=30, 50,$ and $70^\circ C$). Other experimental conditions: $[Phenol]_0 = 10.6$ mM, $[H_2O_2]_0 = 190$ mM, $pH_0 = 5.0$. In all cases, lines indicate the proposed model (Eqs. (7)–(9)) using the coefficients showed in Table 2.



According to Reactions (3) and (4), during the second phase of the phenol oxidation, 8–11 mol of H_2O_2 are consumed per mol of C_6 -intermediate oxidized. Once again, the actual value is a function of the reaction conditions. Because in R3 and R4 all intermediates are oxidized to CO_2 , both reactions contribute to the TOC consumption of the solution. Finally, the overall oxidation of phenol by H_2O_2 can be obtained by the combination of Reactions (1), (3), (2), and (4)



Taking into account the high complexity of the pathway of phenol oxidation above mentioned, and the numerous reactions concerning the several radicals (mainly hydroxide, hydroperoxide, and superoxide radicals) that are present in Fenton and Fenton-like systems [8], a lumped kinetics is usually enough for practical purposes. The model for the oxidation of phenol by H_2O_2 proposed in the present work comprises two types of organic carbon. The fast oxidizable organic carbon (S_F) may include all carbon atoms that constitute the fast oxidizable molecules, such as phenol, catechol, and hydroquinone, for example.

The oxidation of this carbon fraction by H_2O_2 produces a slow oxidizable organic carbon (S_S); this carbon fraction may include 2,5-dioxo-3-hexenedioic, and muconic as well as other organic acids. Then, in the presence of H_2O_2 , S_S is further oxidized to CO_2 . If S_F and S_S are expressed in C-mol units, then the overall stoichiometry corresponding to these reactions are the following



where R_F and R_S are the rates corresponding to reactions (6) and (7), respectively. Because these reactions are expressed in C-mol units, the complete oxidation of S_F produces one mol of CO_2 . Although the stoichiometric coefficients ν_F and ν_S can adopt any value, the overall oxidation of phenol by H_2O_2 (R5) imposes the following restriction to these coefficients

$$\nu_F + \nu_S = \frac{14}{6} \text{ mol}H_2O_2/\text{C-mol} \quad (1)$$

Due to peroxide consuming side reactions, the actual H_2O_2 consumption is higher than the stoichiometric value corresponding to R5. In Fenton and Fenton-like systems, these side reactions are mainly due to the presence of hydroxide radicals that catalyze the decomposition of hydrogen peroxide producing molecular oxygen. Although the catalytic decomposition of H_2O_2 is quite complex and involves several reaction steps [48], the overall decomposition of H_2O_2 can be represented as follows



where R_p is the decomposition rate of peroxide. At this point, it worth to note that a similar modeling approach was used by Guo and Al-Dahhan [21], and Zazo et al. [20]. However, in both cases those authors assume that during the first oxidation step of phenol (R6 in the present model) a given amount of CO_2 is released, decreasing the TOC of the solution. Conversely, in reaction R6 of the present model the overall TOC value is constant, in accordance with the phenol oxidation pathways reported by other authors [42–47]. Moreover, Zazo et al. [20] developed a model for the TOC evolution only. Finally, other important difference between the model proposed by Guo and Al-Dahhan [21] and the model developed in the present work is the relation between the stoichiometric coefficients ν_F and ν_S depicted in Eq. (1).

To obtain the kinetic expressions corresponding to R_F , R_S , and R_p , the pseudo-first-order constants corresponding to the initial decomposition rate of TOC and H_2O_2 were calculated from the plot on a log-scale of TOC and H_2O_2 concentrations as a function of time (Supplementary data, Figs. SD3 and SD4). Obtained results demonstrate that the initial decomposition rate of TOC and H_2O_2 could be approximated by a pseudo-first-order kinetic law with respect to TOC and H_2O_2 concentrations, respectively.

$$\ln([TOC]/[TOC]_0) = -k_{appTOC}t \quad (2)$$

$$\ln([H_2O_2]/[H_2O_2]_0) = -k_{app}t \quad (3)$$

Table 1
Examples of phenol (X_{Phenol}) and TOC (X_{TOC}) conversions, pH, and color of the reaction mixture at 240 min obtained at different tested operating conditions. In all cases $[\text{Phenol}]_0 = 10.6 \text{ mM}$, $[\text{H}_2\text{O}_2]_0 = 190 \text{ mM}$.

T ($^{\circ}\text{C}$)	Cu_T (mg/L)	X_{Phenol} (%)	X_{TOC} (%)	pH_{min}	pH_{final}	Final color
30	20	77	15	3.4	3.4	Dark brown
30	100	90	22	3	3	Brown
30	200	95	30	3	3	Brown
50	5	85	14	2.6	2.6	Dark brown
50	20	96	30	2.7	3	Brown
50	60	100	57	2.9	3	Brown
50	100	100	62	3	3	Brown
50	200	100	83	2.6	3	Brown
50	800	96	84	2.4	3.6	Brown
70	5	100	35	2.8	2.8	Brown
70	20	100	60	2.6	2.8	Transparent dark amber
70	60	100	84	2.5	3	Almost colorless
70	100	100	91	2.5	3.5	Almost colorless
70	200	100	91	2.3	3.7	Almost colorless

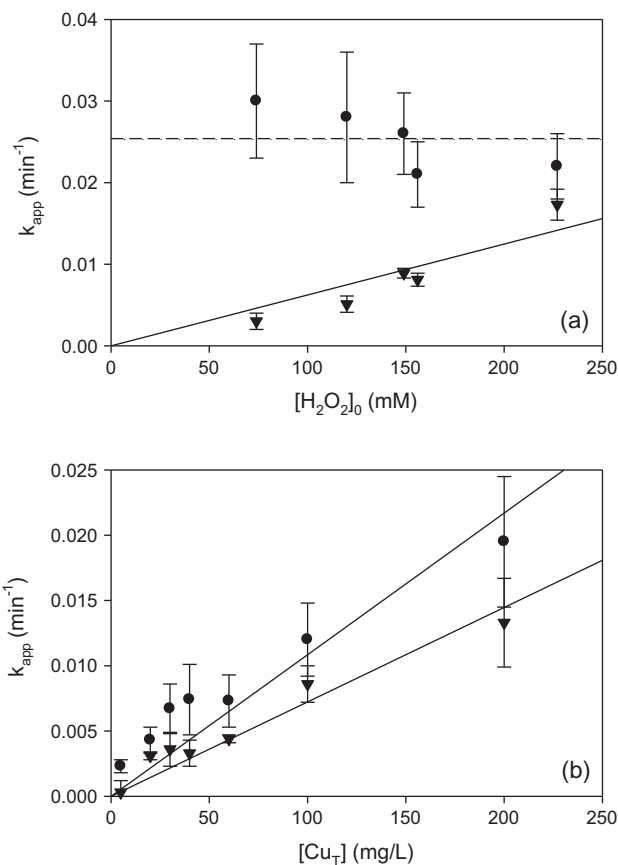


Fig. 5. Effect of (a) the initial H_2O_2 concentration ($[\text{Cu}_T] = 200 \text{ mg/L}$), and (b) the total copper concentration ($[\text{H}_2\text{O}_2]_0 = 190 \text{ mM}$) on the pseudo-first-order rate constant (k_{app}) corresponding to the consumption of TOC (triangles), and H_2O_2 (circles). Other experimental conditions: $[\text{Phenol}]_0 = 10.6 \text{ mM}$, $\text{pH}_0 = 5$, and $T = 50 \text{ }^{\circ}\text{C}$.

where k_{appTOC} and $k_{\text{appH}_2\text{O}_2}$ are the pseudo-first-order rate constants of the initial rate of decomposition of TOC and H_2O_2 , respectively. Fig. 5 shows that k_{appTOC} was proportional to H_2O_2 and copper concentrations. Based on these results, the following expressions for the rates corresponding to reactions R6 and R7 (R_F , R_S) were proposed:

$$R_F = k_F[S_F][\text{Cu}_T][\text{H}_2\text{O}_2] \quad (4)$$

$$R_S = k_S[S_S][\text{Cu}_T][\text{H}_2\text{O}_2] \quad (5)$$

Fig. 5 shows that the pseudo-first-order rate constant corresponding to the H_2O_2 decomposition ($k_{\text{appH}_2\text{O}_2}$) depended on the total Cu concentration (Cu_T) in the reaction mixture. However, $k_{\text{appH}_2\text{O}_2}$ was approximately constant with respect to the initial H_2O_2 concentration. These results are in accordance with those reported by other authors with regard to the catalytic decomposition of hydrogen peroxide by ferric iron [48,49]. Thus, the following expression was proposed to represent the catalytic decomposition rate of peroxide by copper (R_P).

$$R_P = k_P[\text{Cu}_T][\text{H}_2\text{O}_2] \quad (6)$$

According to reactions R6–R8, and taking into account the proposed expressions corresponding to R_F , R_S , and R_P (Eqs. (4)–(6)), the decomposition rate of S_F , S_S and H_2O_2 can be represented by the following coupled ordinary differential equations

$$\frac{d[S_F]}{dt} = -k_F[S_F][\text{Cu}_T][\text{H}_2\text{O}_2] \quad (7)$$

$$\frac{d[S_S]}{dt} = \{k_F[S_F] - k_S[S_S]\}[\text{Cu}_T][\text{H}_2\text{O}_2] \quad (8)$$

$$\frac{d[\text{H}_2\text{O}_2]}{dt} = -\{v_F k_F[S_F] + v_S k_S[S_S] + k_P\}[\text{Cu}_T][\text{H}_2\text{O}_2] \quad (9)$$

Because the units used to express the primary experimental data were TOC in mgC/L, phenol, and hydrogen peroxide in mM, total copper (Cu_T) in mgCu/L, and time in min, the developed model was also expressed using these units. Thus, if S_F and S_S are expressed in mgC/L, TOC concentration of the solution can be calculated as follows

$$[\text{TOC}] = [S_F] + [S_S] \quad (10)$$

and the restriction regarding v_F , and v_S (Eq. (1)) expressed in these units is

$$v_F + v_S = \frac{14}{72} \text{ molH}_2\text{O}_2/\text{gC} \quad (11)$$

Besides, assuming that the fast oxidizable organic carbon (S_F) is represented mainly by phenol, the phenol concentration can be calculated as follows

$$[\text{Ph}] = \frac{[S_F]}{72} \quad (12)$$

where 72 (gC/mol) is the carbon mass in one mol of phenol.

3.5. Model calibration

The software GEPASI was used to fit the model developed (Eqs. (7)–(9)) to the profiles of hydrogen peroxide, TOC, and phenol

concentrations as a function of time obtained at different Cu_T (5–800 mg/L), and initial H_2O_2 concentrations (75–230 mM). Although the model has five coefficients, it worth to note that considering the restriction regarding v_F , and v_S , only four coefficients were fitted. Fitting results are depicted in Table 2. Details concerning the implementation of the proposed model in GEPASI, and other fitting details can be found in the Supplementary data.

Figs. 1–4 show that the fitted model could adequately describe TOC, hydrogen peroxide, and phenol conversions as a function of time during the cupro-Fenton oxidation of phenol over a wide range of experimental conditions. Table 2 shows that calculated conversions of TOC and H_2O_2 were close to the experimental values, with average absolute errors lower than 8%; in the case of phenol conversions, average absolute errors were lower than 12.1%.

According to reaction R6, v_F represents the amount H_2O_2 consumed per unit of S_F oxidized to S_S ; for the three tested temperatures the average value corresponding to v_F was 0.043 mol/gC. Based on this average v_F value, and taking into account the carbon content of phenol (72 gC/mol), it was concluded that during the first oxidation step, 3.1 mol of H_2O_2 were consumed per mol of phenol oxidized. This result is in accordance with reaction R1 (phenol to muconic acid), in which 3 mol of H_2O_2 are consumed per mol of phenol oxidized, providing a strong validation of the proposed model (Fig. 6a).

Based on the values of k_F , k_S , and k_P obtained at different temperatures (Table 1), apparent activation energies corresponding to the reactions R6–R8 were calculated as the slopes of $\ln(k)$ as a function of $1/T$. Fig. 6b shows that reactions R6, and R7 had similar activation energies, being 25.2, and 20.9 kcal/mol, respectively. Nichela et al. [8] reported an apparent activation energy of 27.3 kcal/mol corresponding to the initial degradation rate of the nitrobenzene oxidation by a cupro-Fenton reaction at temperatures above 35 °C. The activation energy reported by those authors is similar to the activation energy corresponding to R6 of the present work. Moreover, this value is close to the activation energy corresponding to the reaction between Cu(II) and hydrogen peroxide to form Cu(I) and the hydroperoxide radical [50], supporting the hypothesis that this reaction is one of the rate limiting steps in cupro-Fenton systems [8].

The activation energy corresponding to the decomposition of hydrogen peroxide (R8) was 8.9 kcal/mol, being this activation energy much lower than those corresponding to R6 and R7. The increase of temperature favored reactions R6, and R7 with respect to R8 (Fig. 6b), suggesting that high temperatures are advantageous in the oxidation of phenol by the cupro-Fenton reaction. Fig. 7 shows that rates of TOC conversion (Fig. 7a), and hydrogen peroxide consumption (Fig. 7b) increased with temperature. Besides, the consumption of hydrogen peroxide to achieve a TOC conversion of 30% at 30 °C was more than twice the consumption at 50 °C. However, a further increment in the operation temperature from 50 to 70 °C did not caused a noticeable decrease on the hydrogen peroxide consumption for the same TOC conversion (Fig. 7c). For example, the time necessary to achieve a TOC conversion of 80% was 180 min at 50 °C, but only 15 min at 70 °C (Fig. 7a);

Table 2

Rate constants (k_F , k_S , k_P), stoichiometric coefficients (v_F , v_S), and average absolute error (AAE) in the percentage conversions of TOC, H_2O_2 , and phenol predicted by the proposed model (Eqs. (7)–(9)).

T (°C)	$k_F \times 10^{5a}$	$k_S \times 10^{8a}$	$k_P \times 10^{5b}$	v_F^c	v_S^c	AAE		
						X_{TOC}	$X_{H_2O_2}$	X_{Phenol}
30	0.34 ± 0.03	7.26 ± 0.11	1.37 ± 0.05	0.044 ± 0.007	0.150 ± 0.003	4.4	7.8	12.1
50	7.92 ± 0.57	10.4 ± 0.03	1.59 ± 0.01	0.029 ± 0.003	0.165 ± 0.001	4.2	3.3	7.1
70	43.3 ± 7.88	56.6 ± 0.4	7.91 ± 0.12	0.056 ± 0.015	0.140 ± 0.002	6.0	5.8	2.1

^a $mM^{-1} L mgCu^{-1} min^{-1}$.

^b $L mgCu^{-1} min^{-1}$.

^c $mol gC^{-1}$.

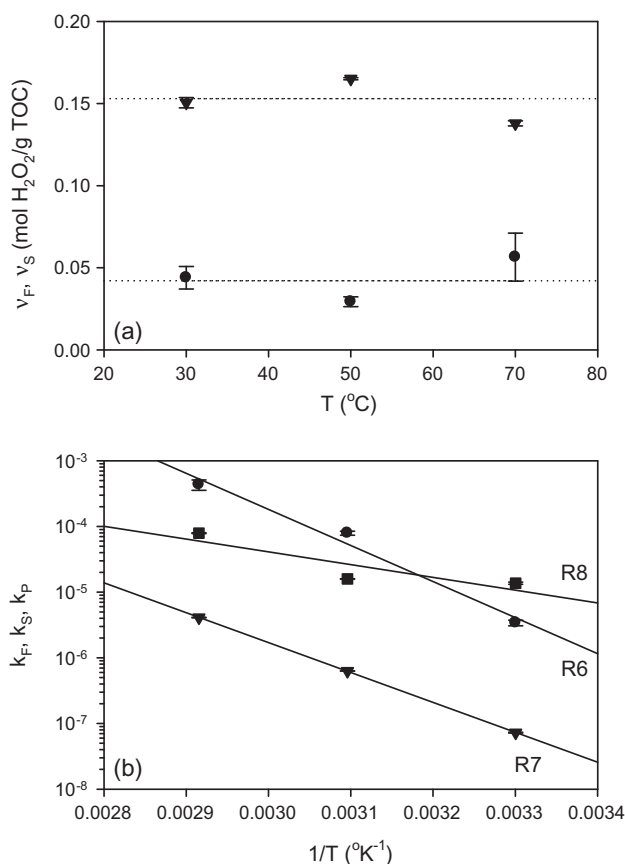


Fig. 6. (a) Effect of temperature on the stoichiometric coefficients v_F (circles) and v_S (triangles) corresponding to the reactions R6 and R7, respectively. Dotted lines denote the calculated v_F and v_S values assuming that reaction R1 represents the oxidation of phenol to muconic acid. (b) Arrhenius plots corresponding to the reactions R6 (circles), R7 (triangles), and R8 (squares).

in both cases, a similar hydrogen peroxide consumption was obtained (Fig. 7b). Thus, from a practical point of view, obtained results in the present work demonstrate that increasing the operation temperature from 50 to 70 °C allows process intensification in terms of higher processing capacities, or the design of smaller reactors without increasing the costs associated with the addition of hydrogen peroxide.

3.6. Operation of a cupro-Fenton sequencing batch reactor (CFSBR)

One of the main problems associated with the use of the cupro-Fenton reaction is the toxicity of Cu(II). For this reason, copper must be removed from the treated wastewater prior discharging to a receiving body water. Moreover, in order to reduce operation costs, it is advisable to recover the used copper in the oxidation reaction. In this work, alkaline precipitation with NaOH was used to precipitate and recover the Cu(II).

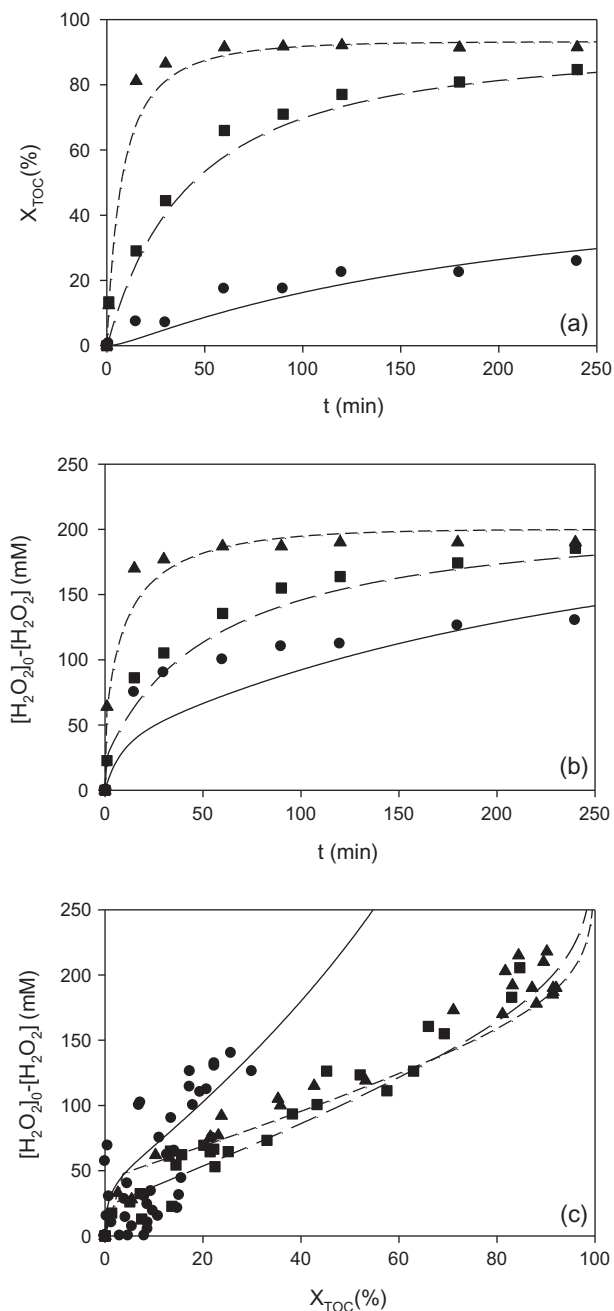


Fig. 7. (a) TOC conversion (X_{TOC}), and (b) hydrogen peroxide consumption as a function of time, and (c) hydrogen peroxide consumption as a function of the TOC conversion obtained at different temperatures ($^{\circ}C$): 30 (circles, continuous lines), 50 (squares, long dashed lines), 70 (triangles, short dashed lines). Experimental conditions: $[Phenol]_0 = 10.6$ mM, $[H_2O_2]_0 = 200$ mM, $[Cu_T] = 200$ mg/L, $pH_0 = 5.0$. In all cases, lines indicate the proposed model (Eqs. (7)–(9)) using the coefficients showed in Table 2.

3.6.1. Optimal pH for Cu(II) precipitation

In a first set of experiments, oxidation of phenol solutions (10.6 mM) at two temperatures was carried out using 200 mg/L of Cu(II), and 190 mM of H_2O_2 . At $T = 50$ $^{\circ}C$, the final reaction time was 240 min; when 70 $^{\circ}C$ was tested, the final reaction time was 90 min. In both cases, the reaction was drastically decelerated by cooling the reactor in a water bath to room temperature. Results demonstrate that under both tested conditions, phenol conversions were almost complete. TOC conversions at 50 $^{\circ}C$ (240 min) were close to 80%, whereas at 70 $^{\circ}C$ (90 min) conversions of about 90% were obtained. Although TOC conversions at both tempera-

tures were quite acceptable, at 50 $^{\circ}C$ (240 min) the color of the reaction mixture was brown due to the presence of colored cation complexes and phenol condensation products [40,41]. Conversely, the reaction mixture obtained at 70 $^{\circ}C$ (90 min) was almost transparent, in accordance with its higher mineralization degree.

In order to determine the optimal pH for copper precipitation, both reaction mixtures (50 $^{\circ}C$, 240 min; 70 $^{\circ}C$, 90 min) were divided in aliquots of 50 mL. Then, pH of these samples was adjusted to a desired value using NaOH (1 M) under soft continuous stirring. When the desired pH value was reached, samples were centrifuged at 4200 rpm for 30 min to remove the precipitated copper and total copper concentration in the supernatant (Cu_{TS}) was measured. The optimal precipitation pH corresponding to the reaction mixture obtained at 50 $^{\circ}C$ (240 min) was 8; in this case, the minimum copper concentration in the supernatant was 6.3 mg/L. With the sample obtained at 70 $^{\circ}C$ (90 min), the optimal precipitation pH was 10 and the minimum copper concentration in the supernatant was 0.4 mg/L. Best results were obtained when oxidation tests were performed at 70 $^{\circ}C$ (90 min) followed by a precipitation step at pH 10 (Supplementary data, Table SD2). These conditions ensured Cu(II) concentrations in the supernatant below the limits established by EPA, and WHO [12,13].

Differences regarding the optimal precipitation pH could be due to the presence of different oxidation intermediates at each experimental condition. Besides the hydroxide complexes, as a general rule Cu(II) can also be complexed by a great number of organic ligands [51], including some of the reported intermediates obtained during the oxidation of phenol [42–47]. The formation of these complexes altered the Cu(II) solubility and also the optimal precipitation pH. Because the distribution of these intermediates is a function of the oxidation conditions, the optimal precipitation pH is also a function of these conditions. Moreover, other factors also affect the precipitation of Cu(II) by NaOH. For example, Marani et al. [52] observed that at base/Cu(II) molar ratios lower than 1.5, the slow addition of NaOH to dilute $CuSO_4$ solutions produces blue precipitate of posnjakite ($CuSO_4 \cdot 3Cu(OH)_2 \cdot H_2O$) or posnjakite and brochantite ($CuSO_4 \cdot 3Cu(OH)_2$) mixtures. At higher base/Cu(II) molar ratios and $pH > 7.3$, the formation of a dark precipitate of tenorite (CuO) was observed. Jiang et al. [53] demonstrated that in the presence of carbonates, other green/blue solid phases, such as malachite ($Cu_2(OH)_2CO_3$) and azurite ($Cu_3(OH)_2(CO_3)_2$) can also appear. CO_2 also exerts negative effect on the copper removal efficiency due to the formation of the soluble compound $Cu(CO_3)_2^{2-}$. However, because the total carbonate concentration is a function of the gas–liquid mass transfer coefficient, the atmospheric CO_2 partial pressure, and the actual pH of the solution [54], the net effect of CO_2 on the solubility of Cu(II) is difficult to predict.

3.6.2. Effect of the employed Cu(II) separation techniques on the performance of the cupro-Fenton sequencing batch reactor (CFSBR)

Based on the above mentioned results (Section 3.6.1), the CFSBR was operated at 70 $^{\circ}C$, with an initial Cu(II) concentration of 200 mg/L, and initial H_2O_2 concentration of 190 mmol/L. After 90 min, the reactor was cooled to room temperature; then, few drops of NaOH (1 M) were added up to pH 10. The addition of NaOH generated a precipitate that was further separated by decantation or centrifugation. When a decantation procedure was used, the whole reaction mixture ($V_0 = 170$ mL) was left in a decanting ampoule for 1 h. Then, 80 mL of the supernatant (V_S) were carefully extracted to avoid turbulences and the remnant volume (e.g., $V_0 - V_S$) was recycled to the reactor. When centrifugation was used, the reaction mixture was centrifuged at 4200 rpm for 30 min. Because a lower sludge volume was obtained using centrifugation in comparison with decantation, 140 mL of the supernatant (V_S) could be extracted and a smaller remnant volume was

recycled to the reactor. In both cases, to dissolve the Cu(II) precipitate, pH of the recycled sludge was adjusted to 5 by adding a few drops of H₂SO₄ (2 M). Then, a volume equivalent to V_S of a phenol solution of appropriate concentration was added to obtain an initial phenol concentration of 10.6 mM. Finally, a new reaction cycle started with the addition of 3.3 mL of hydrogen peroxide (30% wt/wt).

Five consecutive batch tests were performed using decantation or centrifugation as the Cu(II) separation technique. In both cases, phenol conversions were almost close to 100%. Fig. 9a shows that with both separation techniques, TOC values at the end of the reaction phase (TOC_f) were between 90 and 120 mgC/L (which represented TOC conversions of 85–90%). Moreover, a slight increase of the hydrogen peroxide concentrations as a function of the operation cycle was observed due to lower reaction conversions (Fig. 9b). However, it must be noted that remnant hydrogen peroxide concentrations were in all cases less than 8% of the initial value. Fig. 9c shows that during the precipitation step not only the Cu(II) was separated from the solution, but also part of the organic carbon; for this reason, TOC values of the supernatant (TOC_S) were lower than TOC_f (Fig. 9a). When decantation was used as the separation method of the cupro-Fenton sludge, the total copper concentration in the supernatant (Cu_{TS}) increased from 4 to 28 mg/L as a function of the operation cycle (Fig. 9d). This effect could be related to the higher residual H₂O₂ concentration that generates air bubbles in the separating ampoule leading to the deterioration of sludge settleability [55]. In the case of centrifugation, a similar trend was observed; however, in this case, Cu_{TS} concentrations of about one order of magnitude lower were achieved, being Cu_{TS} values always lower than 1 mg/L.

It worth to mention that within the five consecutive runs, TOC and phenol conversions were almost constant. However, Fig. 9 shows an evident deterioration of the settling characteristics of the cupro-Fenton sludge as a function of the operation cycle. For example, when decantation was used as the separation technique, the ratio between the total copper concentration in the reactor (Cu_T) and the total copper in the supernatant (Cu_{TS}) gradually increased from 0.02 to 0.16 (Fig. 9a). A similar trend was obtained with regard to the ratio between TOC values at the end of the reaction phase (TOC_f) and TOC in the supernatant (TOC_S) using both separation techniques (Fig. 9b). This behavior was due to the relationship between the oxidation conditions (e.g., differences in copper concentrations) and the distribution of the oxidation intermediates, as it was commented in the previous section (Section 3.6.1). Lower copper concentrations may lead to the formation of a different intermediate distribution; thus, higher amounts of Cu(II) could be complexed by those formed ligands. These Cu(II) complexes determine a gradual decrease of Cu_T concentrations in the reactor due to the presence of higher Cu(II) concentrations in the supernatant. As a result, the increase of the complexed fraction of Cu(II) may lead to a gradual decrease of the TOC, H₂O₂, and phenol conversions in long-term operation of the CFSBR. In this sense, the performance of the CFSBR could be more stable if centrifugation instead of a decantation method is used to recover the Cu(II).

3.6.3. Modeling the cupro-Fenton sequencing batch reactor (CFSBR)

In order to obtain accurate predictions of the CFSBR performance, initial concentrations of a given operation cycle must be expressed as a function of the concentration at the end of the preceding cycle. For example, if Cu_{T(i)} represents the total Cu(II) concentration in the reactor at the beginning of a given cycle *i*, then Cu_{T(i+1)} can be calculated as follows

$$\text{Cu}_{T(i+1)} = \text{Cu}_{T(i)} - \frac{V_S}{V_0} \text{Cu}_{TS(i)} \quad (13)$$

where Cu_{TS(i)} represents the Cu(II) concentration in the supernatant after the precipitation with NaOH corresponding to the cycle *i*, V₀ is the reactor volume, and V_S the treated supernatant volume during each cycle. In the case of TOC, assuming that the added phenol stock solution was devoid of the slow oxidizable compound (S_S), the initial S_S concentration (S_{S0}) corresponding to the cycle (*i* + 1) is

$$S_{S0(i+1)} = S_{Sf(i)} - \frac{V_S}{V_0} S_{SS(i)} \quad (14)$$

where S_{Sf(i)}, and S_{SS(i)} refer to the concentrations of S_S at the end of the reaction phase, and in the supernatant, respectively. Taking into account that under the selected operation conditions (70 °C, 90 min) the conversion of S_F was complete, the initial S_F concentration (S_{F0}) was a function of V₀, V_S, and the concentration of the phenol stock solution (S_{FSt})

$$S_{F0(i)} = \frac{V_S}{V_0} S_{FSt} \quad (15)$$

Conversely to Cu_T, and S_S, the initial S_F concentration is not depended on the operation cycle number (*i*). Although V₀ was constant (V₀ = 170 mL), V_S depended on the separation technique. Thus, the concentration of the phenol stock solution (S_{FSt}) was selected in order to obtain S_{F0} = 766 mgC/L (10.6 mM of phenol) for both separation methods. With regard to the hydrogen peroxide, due to the addition of NaOH for the alkaline precipitation of Cu(II), the hydrogen peroxide concentration after the separation step was negligible. For this reason, a similar expression than Eq. (15) can be deduced to calculate the initial H₂O₂ concentration corresponding to the reaction phase; in this case, [H₂O₂]₀ = 190 mM.

Although for a given cycle, S_{Sf} can be calculated based on the initial conditions using the model proposed in the present work (Eqs. (7)–(9)), Eqs. (13) and (14) demonstrate that initial conditions corresponding to S_{S0(i+1)}, and Cu_{T(i+1)} are a function of S_{SS(i)} and Cu_{TS(i)}. In order to take into account the effect of the separation technique (decantation or centrifugation) on the performance of the CFSBR, the ratios Cu_{TS}/Cu_T, and TOC_S/TOC_f were calculated for each operation cycle (Fig. 9). Because under the tested conditions phenol is rapidly converted to S_S, TOC values at the end of the reaction phase (TOC_f) corresponded to S_S; thus, the ratio TOC_S/TOC_f represented the ratio S_{SS}/S_F. Fig. 9 shows that Cu_{TS}/Cu_T, and TOC_S/TOC_f increased as a function of the cycle; also, those ratios depended on the technique used to recover the cupro-Fenton sludge (decantation or centrifugation). According to Fig. 9, both Cu_{TS}/Cu_T, and TOC_S/TOC_f ratios (ε_{Cu*i*}, ε_{TOC*i*}) as a function of the operation cycle (*i*) can be estimated by the following empirical equation

$$\varepsilon_i = 1 - \alpha e^{-\beta i} \quad (16)$$

where the values corresponding to the constants α, and β depended on the separation techniques (decantation or centrifugation) employed in this work. The term (1 - ε_{Cu*i*}) represents the separation efficiency of Cu(II) by a given separation method; thus, high values of β indicate a rapid deterioration of the settling characteristics as a function of the operation cycle. Conversely, combinations of low values of β with high α values indicate a good separation procedure. Eq. (16) was fitted to the data depicted in Fig. 9, obtaining quite acceptable results; Table 3 shows the obtained constants (α, β) corresponding to both separation processes. As it was expected,

Table 3
Coefficients α, β of Eq. (15) corresponding to the separation of Cu(II) and TOC by decantation or centrifugation (for more details see the text).

Variable	Coefficient	Decantation	Centrifugation
Cu(II)	α	1.03 ± 0.01	0.99 ± 0.01
	β	(40 ± 4) × 10 ⁻³	(2.3 ± 0.8) × 10 ⁻⁴
TOC	α	0.84 ± 0.07	0.93 ± 0.07
	β	0.095 ± 0.028	0.079 ± 0.027

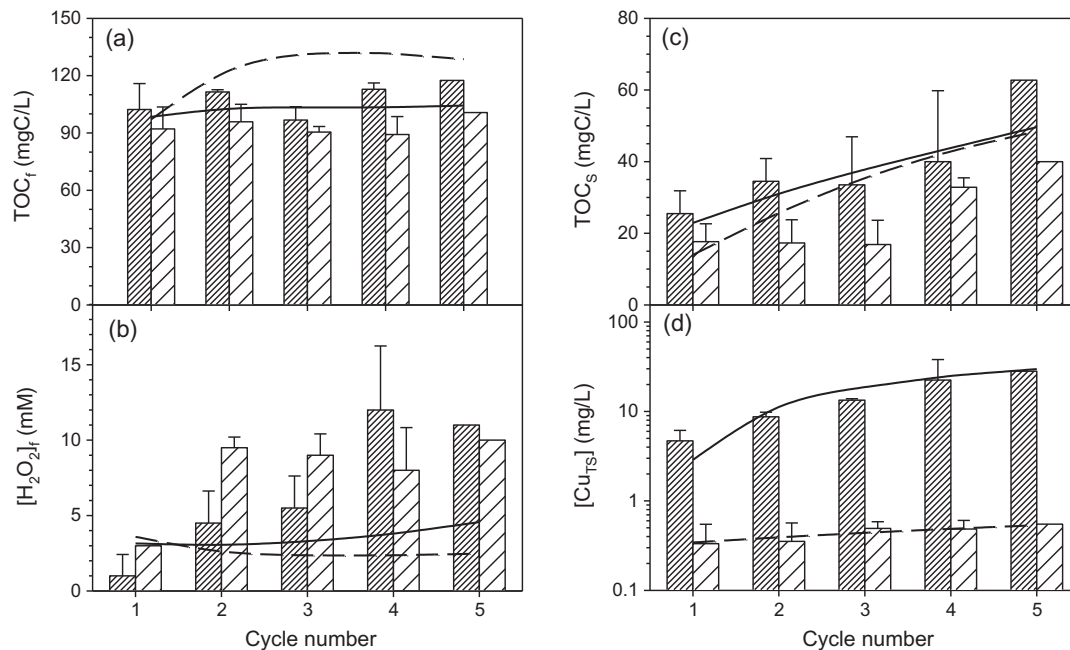


Fig. 8. Performance of the CFSBR as a function of the operation cycle. TOC (a), and hydrogen peroxide concentration (b) at the end of the reaction phase; TOC (c), and total copper concentration (d) in the supernatant after the separation of the Fenton sludge by decantation (fine patterns, continuous lines) or centrifugation (coarse patterns, dashed lines). Operation conditions of the CFSBR: $[\text{Phenol}]_0 = 10.6 \text{ mM}$, $[\text{H}_2\text{O}_2]_0 = 190 \text{ mM}$, $[\text{Cu}_T]$ of the first operation cycle = 200 mg/L , $\text{pH}_0 = 5.0$, precipitation $\text{pH} = 10$. In all cases, lines indicate the model proposed in this work (Eqs. (7), (8), (9), (13), (14), and (15)) using the coefficients showed in Tables 2 and 4.

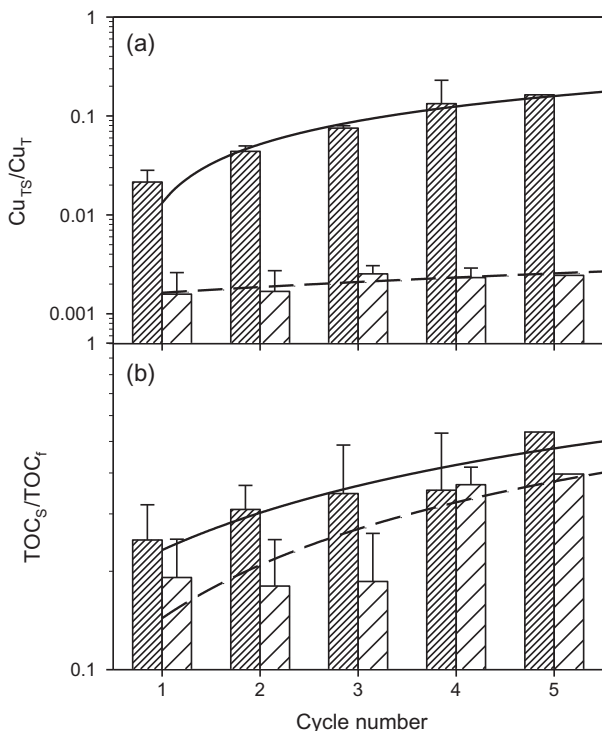


Fig. 9. Effect of the cycle number on (a) the ratio between the total copper concentration in the supernatant after the separation step (Cu_{TS}) and the total copper concentration in the reactor (Cu_T), and on (b) and the ratio between TOC in the supernatant after the separation step (TOC_s) and TOC at the end of the reaction phase (TOC_f), obtained using decantation (fine patterns, continuous lines) or centrifugation (coarse patterns, dashed lines). Operation conditions of the CFSBR: $[\text{Phenol}]_0 = 10.6 \text{ mM}$, $[\text{H}_2\text{O}_2]_0 = 190 \text{ mM}$, $[\text{Cu}_T]$ of the first operation cycle = 200 mg/L , $\text{pH}_0 = 5.0$, precipitation $\text{pH} = 10$. In all cases, lines indicate the results of Eq. (16) using the coefficients depicted in Table 4.

obtained coefficients indicate that centrifugation rather than decantation was a better method to separate Cu(II) from the treated solution.

To simulate the performance of the CFSBR, the reaction phase was represented by the kinetic model for the cupro-Fenton oxidation of phenol by hydrogen peroxide developed in the present work (Eqs. (7)–(9)). Then, Eq. (16) was used to represent the separation step and the initial concentrations of Cu_T and S_5 corresponding to the next operation cycle were calculated using Eqs. (13) and (14), respectively. Finally, S_{F0} and H_2O_{20} were considered constants, as it was previously described in the present section.

Fig. 8 shows that for both separation methods a satisfactory accordance between the model and the experimental results was obtained. The maximum difference between experimental and calculated TOC values was 42 mgC/L (Fig. 9a), which represented 5% of the initial TOC. Although Fig. 9b shows that the model tends to overestimate the hydrogen peroxide consumption, the maximum difference between experimental and calculated H_2O_2 conversions values was 4.3%. With regard to the effluent quality, the model also adequately predicts TOC and Cu_T concentrations in the supernatant after the separation step using both (decantation or centrifugation) methods. However, centrifugation was the only tested separation method that ensured a copper concentration in the supernatant below the discharge limit established by EPA, and WHO [12,13].

4. Conclusions

Phenol can be efficiently mineralized using the homogeneous cupro-Fenton reaction. TOC conversions increased with elevated temperatures and hydrogen peroxide concentrations. High temperatures increased the phenol oxidation reaction rate more than the hydrogen peroxide decomposition rate. For this reason, rising the temperature from 30 to $70 \text{ }^\circ\text{C}$ allows reactors with higher processing capacities without increasing the costs associated with the addition of higher amounts of hydrogen peroxide.

A kinetic model based on the phenol oxidation pathway reported by other authors was developed. The effect of peroxide scavenger reactions was also included. The proposed model adequately represents TOC, hydrogen peroxide, and phenol conversions as a function of time over a wide range of experimental conditions.

Finally, to overcome toxicity issues related with the discharge of copper and with the purpose of decreasing the operation costs, the homogeneous catalyst was recovered by alkaline precipitation with NaOH and used in subsequent reactions with minor changes in mineralization and reactants depletion profiles. These outcomes were also predicted by a mathematical model that includes both reaction and separation steps.

Appendix A. Supplementary material

Supplementary data associated with this article can be found, in the online version, at <http://dx.doi.org/10.1016/j.cej.2014.04.019>.

References

- [1] E. Neyens, J. Baeyens, A review of classic Fenton's peroxidation as an advanced oxidation technique, *J. Hazard. Mater.* B98 (2003) 33–50.
- [2] P.R. Gogate, A.B. Pandit, A review of imperative technologies for wastewater treatment I: oxidation technologies at ambient conditions, *Adv. Environ. Res.* 8 (2004) 501–551.
- [3] L.F. Liotta, M. Gruttadauria, G. Di Carlo, G. Perrini, V. Librando, Heterogeneous catalytic degradation of phenolic substrates: catalysts activity, *J. Hazard. Mater.* 162 (2009) 588–606.
- [4] F.L.Y. Lam, A.C.K. Yip, X. Hu, A high performance bimetallic catalyst for photo-Fenton oxidation of Orange II over a wide pH range, *Ind. Eng. Chem. Res.* 46 (2007) 3328–3333.
- [5] S. Navalon, M. Alvaro, H. García, Heterogeneous Fenton catalysts based on clays, silicas and zeolites, *Appl. Catal. B – Environ.* 99 (2010) 1–26.
- [6] D. Mantzavinos, Removal of cinnamic acid derivatives from aqueous effluents by Fenton-like processes as an alternative to direct biological treatment, *Water Air Soil Pollut. Focus* 3 (2003) 211–221.
- [7] D. Mantzavinos, Removal of benzoic acid derivatives from aqueous effluents by the catalytic decomposition of hydrogen peroxide, *Trans. IChemE* 81-B (2003) 99–106.
- [8] D.A. Nichela, A.M. Berkovic, M.R. Costante, M.P. Juliarena, F.S. García, Einschlag, Nitrobenzene degradation in Fenton-like systems using Cu(II) as catalyst. Comparison between Cu(II)- and Fe(III)-based systems, *Chem. Eng. J.* 228 (2013) 1148–1157.
- [9] I.U. Castro, F. Stüber, A. Fabregat, J. Font, A. Fortuny, C. Bengoa, Supported Cu(II) polymer catalysts for aqueous phenol oxidation, *J. Hazard. Mater.* 163 (2009) 809–815.
- [10] J. Prasad, J. Tardio, H. Jani, S.K. Bhargava, D.B. Akolekar, S.C. Grocott, Wet peroxide oxidation and catalytic wet oxidation of stripped sour water produced during oil shale refining, *J. Hazard. Mater.* 146 (2007) 589–594.
- [11] L.C. Friedrich, C.L. de Paiva, S. Zanta, A. Machulek Jr., V. de Oliveira Silva, F.H. Quina, Interference of inorganic ions on phenol degradation by the Fenton reaction, *Sci. Agric.* 69–6 (2012) 347–351.
- [12] EPA, Basic information about copper in drinking water, in: United States Environmental Protection Agency.
- [13] WHO, Copper in drinking-water background document for development of WHO guidelines for drinking-water quality, in: World Health Organization, 2004.
- [14] G. Cao, M. Sheng, W. Niu, Y. Fei, D. Li, Regeneration and reuse of iron catalyst for Fenton-like reactions, *J. Hazard. Mater.* 172 (2009) 1446–1449.
- [15] A. Bach, H. Shemer, R. Semiat, Kinetics of phenol mineralization by Fenton-like oxidation, *Desalination* 264 (2010) 188–192.
- [16] E. Khan, W. Wirojanagud, N. Sermsai, Effects of iron in Fenton reaction on mineralization and biodegradability enhancement of hazardous organic compounds, *J. Hazard. Mater.* 161 (2009) 1024–1034.
- [17] F. Emami, A.R. Tehrani Bagha, K. Gharanjig, F.M. Menger, Kinetic study of the factors controlling Fenton-promoted destruction of a non-biodegradable dye, *Desalination* 257 (1–3) (2010) 124–128.
- [18] J.H. Ramirez, F.M. Duarte, F.G. Martins, C.A. Costa, L.M. Madeira, Modelling of the synthetic dye Orange II degradation using Fenton's reagent: from batch to continuous reactor operation, *Chem. Eng. J.* 148 (2009) 394–404.
- [19] N.S. Inchaurredo, P. Massa, R. Fenoglio, J. Font, P. Haure, Efficient catalytic wet peroxide oxidation of phenol at moderate temperature using a high-load supported copper catalyst, *Chem. Eng. J.* 198–199 (2012) 426–434.
- [20] J.A. Zazo, J.A. Casas, A.F. Mohedano, J.J. Rodríguez, Semicontinuous Fenton oxidation of phenol in aqueous solution A kinetic study, *Water Res.* 43 (2009) 4063–4069.
- [21] J. Guo, M. Al-Dahhan, Catalytic wet oxidation of phenol by hydrogen peroxide over pillared clay catalyst, *Ind. Eng. Chem. Res.* 42 (2003) 2450–2460.
- [22] R.F.F. Pontes, J.E.F. Moraes, A. Machulek Jr., J.M. Pinto, A mechanistic kinetic model for phenol degradation by the Fenton process, *J. Hazard. Mater.* 176 (2010) 402–413.
- [23] N. Villota, F. Mijangos, F. Varona, J. Andrés, Kinetic modelling of toxic compounds generated during phenol elimination in wastewaters, *Int. J. Chem. Reactor Eng.* 5 (2007) A63.
- [24] N. Kang, D.S. Lee, J. Yoon, Kinetic modeling of Fenton oxidation of phenol and monochlorophenols, *Chemosphere* 47 (2002) 915–924.
- [25] H. Debellefontaine, M. Chakchouk, J.N. Foussard, D. Tissot, P. Striolo, Treatment of organic aqueous wastes: wet air oxidation and wet peroxide oxidation, *Environ. Pollut.* 92 (1996) 155–164.
- [26] I.U. Castro, D.C. Sherrington, A. Fortuny, A. Fabregat, F. Stüber, J. Font, C. Bengoa, Synthesis of polymer-supported copper complexes and their evaluation in catalytic phenol oxidation, *Catal. Today* 157 (2010) 66–70.
- [27] R.-M. Liou, S.-H. Chen, Short communication CuO impregnated activated carbon for catalytic wet peroxide oxidation of phenol, *J. Hazard. Mater.* 172 (2009) 498–506.
- [28] K. Maduna Valkaj, A. Katovic, S. Zrnecvic, Investigation of the catalytic wet peroxide oxidation of phenol over different types of Cu/ZSM-5 catalyst, *J. Hazard. Mater.* 144 (2007) 663–667.
- [29] J.A. Zazo, J.A. Casas, A.F. Mohedano, J.J. Rodríguez, Catalytic wet peroxide oxidation of phenol with a Fe/active carbon catalyst, *Appl. Catal. B: Environ.* 65 (2006) 261–268.
- [30] L.S. Clesceri, in: L.S. Clesceri, A.E. Greenberg, A.D. Eaton (Eds.), *Standard Methods for the Examination of Water and Wastewater*, 20th ed., American Public Health Association, Washington, DC, 1998.
- [31] P. Mendes, Gepasi: a software package for modelling the dynamics, steady states and control of biochemical and other systems, *Comput. Appl. Biosci.* 9 (1993) 563–571.
- [32] J.J. Pignatello, E. Oliveros, A. MacKay, Advanced oxidation processes for organic contaminant destruction base on the Fenton reaction and related chemistry, *Crit. Rev. Environ. Sci. Technol.* 36 (1) (2007) 1–84.
- [33] J. De Laat, G.T. Le, B. Legube, A comparative study of the effects of chloride, sulfate and nitrate ions on the rates of decomposition of H₂O₂ and organic compounds by Fe(II)/H₂O₂ and Fe(III)/H₂O₂, *Chemosphere* 55 (2004) 715–723.
- [34] G. Zelmanov, R. Semiat, Phenol oxidation kinetics in water solution using iron(3)-oxide-based nano-catalysts, *Water Res.* 42 (2008) 3848–3856.
- [35] A. Riga, K. Soutsas, K. Ntampeglitis, V. Karayannis, G. Papapolymerou, Comparison of H₂O₂/UV, Fenton, UV/Fenton, TiO₂/UV and TiO₂/UV/H₂O₂ processes, *Desalination* 211 (2007) 72–86.
- [36] P. Bautista, A.F. Mohedano, J.A. Casas, J.A. Zazo, J.J. Rodríguez, Highly stable Fe/γ-Al₂O₃ catalyst for catalytic wet peroxide oxidation, *J. Chem. Technol. Biotechnol.* 86 (2011) 497–504.
- [37] J.A. Zazo, J.A. Casas, A.F. Mohedano, M.A. Gilarranz, J.J. Rodríguez, Chemical pathway and kinetics of phenol oxidation by Fenton's reagent, *Environ. Sci. Technol.* 39 (2005) 9295–9302.
- [38] A. Santos, P. Yustos, S. Rodríguez, E. Simon, F. García-Ochoa, Abatement of phenolic mixtures by catalytic wet oxidation enhanced by Fenton's pretreatment: effect of H₂O₂ dosage and temperature, *J. Hazard. Mater.* 146 (2007) 595–601.
- [39] F. Arena, R. Giovenco, T. Torre, A. Venuto, A. Parmaliana, Activity and resistance to leaching of Cu-based catalysts in the wet oxidation of phenol, *Appl. Catal. B* 45 (2003) 51–62.
- [40] F. Mijangos, F. Varona, N. Villota, Changes in solution color during phenol oxidation by Fenton reagent, *Environ. Sci. Technol.* 40 (2006) 5538–5543.
- [41] M. Reihman, H. Ritter, Synthesis of phenol polymers using peroxidases, *Adv. Polym. Sci.* 194 (2006) 1–49.
- [42] J. Villaseñor, P. Reyes, G. Pecchi, Catalytic and photocatalytic ozonation of phenol on MnO₂ supported catalysts, *Catal. Today* 76 (2002) 121.
- [43] B. Roig, C. Gonzalez, O. Thomas, Monitoring of phenol photodegradation by ultraviolet spectroscopy, *Spectrochim. Acta Part A* 59 (2003) 303.
- [44] M.K. Ramseier, U. von Gunten, Mechanisms of phenol ozonation – kinetics of formation of primary and secondary reaction products, *Ozone Sci. Eng.* 31 (2009) 201.
- [45] E. Mvula, C. von Sonntag, Ozonolysis of phenols in aqueous solution, *Org. Biomol. Chem.* 1 (2003) 1749.
- [46] V.D. Komissarov, Y.S. Zimin, S.L. Khursan, On the mechanism of phenol ozonolysis, *Kinetics Catal.* 47 (2006) 850.
- [47] H.R. Devlin, I.J. Harris, Mechanism of the oxidation of aqueous phenol with dissolved oxygen, *Ind. Eng. Chem. Fundam.* 23 (1984) 387.
- [48] J. De Laat, H. Gallard, Catalytic decomposition of hydrogen peroxide by Fe(III) in homogeneous aqueous solution: mechanism and kinetic modeling, *Environ. Sci. Technol.* 33 (1999) 2726–2732.
- [49] S.-S. Lin, M.D. Guroi, Catalytic decomposition of hydrogen peroxide on iron oxide: kinetics, mechanism, and implications, *Environ. Sci. Technol.* 32 (1998) 1417–1423.
- [50] F.J. Millero, V.K. Sharma, B. Karn, The rate of reduction of copper (II) with hydrogen peroxide in seawater, *Mar. Chem.* 36 (1–4) (1991) 71–83.
- [51] W. Stumm, J.J. Morgan, *Aquatic Chemistry, Chemical Equilibria and Rates in Natural Waters*, third ed., Wiley, New York, 1996. pp 425–513.
- [52] D. Marani, J.W. Patterson, P.R. Anderson, Alkaline precipitation and aging of Cu (II) in the presence of sulfate, *Water Res.* 29 (5) (1995) 1317–1326.
- [53] H.-L. Jiang, J.-H. Tay, S. Tay, Changes in structure, activity and metabolism of aerobic granules as a microbial response to high phenol loading, *Appl. Microbiol. Biotechnol.* 63 (2004) 602–608.
- [54] E.M. Contreras, Carbon dioxide stripping in bubbled columns, *Ind. Eng. Chem. Res.* 46 (19) (2007) 6332–6337.
- [55] H.-C. Yoo, S.-H. Cho, S.-O. Ko, Modification of coagulation and Fenton oxidation processes for cost-effective leachate treatment, *J. Environ. Sci. Health A36* (1) (2001) 39–48.